HHS Public Access

Author manuscript

Wound Repair Regen. Author manuscript; available in PMC 2016 January 08.

Published in final edited form as:

Wound Repair Regen. 2014 ; 22(6): 720–729. doi:10.1111/wrr.12229.

A Modified Collagen Gel Dressing Promotes Angiogenesis in a Pre-Clinical Swine Model of Chronic Ischemic Wounds

Haytham Elgharably, MD, **Kasturi Ganesh, MD**, **Jennifer Dickerson, RVT**, **Savita Khanna, PhD**, **Motaz Abas, BS**, **Piya Das Ghatak, MS**, **Sriteja Dixit, MS**, **Valerie Bergdall, DVM**, **Sashwati Roy, PhD**, and **Chandan K. Sen, PhD**

Departments of Surgery, Davis Heart & Lung Research Institute, Center for Regenerative Medicine and Cell based Therapies and Comprehensive Wound Center, The Ohio State University Wexner Medical Center, Columbus, Ohio 43210

Abstract

We recently performed proteomic characterization of a modified collagen gel (MCG) dressing and reported promising effects of the gel in healing full-thickness excisional wounds. In this work, we test the translational relevance of our aforesaid findings by testing the dressing in a swine model of chronic ischemic wounds recently reported by our laboratory. Full thickness excisional wounds were established in the center of bi- pedicle ischemic skin flaps on the backs of animals. Ischemia was verified by Laser Doppler imaging and MCG was applied to the test group of wounds. Seven days post- wounding, macrophage recruitment to the wound was significantly higher in MCG-treated ischemic wounds. *In vitro*, MCG up-regulated expression of Mrc-1 (a reparative M2 macrophage marker) and induced the expression of anti-inflammatory cytokine IL-10 and of β-FGF. An increased expression of CCR2, a M2 macrophage marker, was noted in the macrophages from MCG treated wounds. Furthermore, analyses of wound tissues 7 days post wounding showed up-regulation of TGF-β, VEGF, vWF, and collagen type I expression in MCG-treated ischemic wounds. At 21 days post-wounding, MCG-treated ischemic wounds displayed higher abundance of proliferating endothelial cells that formed mature vascular structures and increased blood flow to the wound. Fibroblast count was markedly higher in MCG-treated ischemic wound-edge tissue. In addition, MCG-treated wound-edge tissues displayed higher abundance of mature collagen with increased collagen type I:III deposition. Taken together, MCG helped mount a more robust inflammatory response which resolved in a timely manner, followed by an enhanced proliferative phase, angiogenic outcome and post-wound tissue remodeling. Findings of the current study warrant clinical testing of MCG in a setting of ischemic chronic wounds.

INTRODUCTION

Chronic wounds are rarely seen in individuals who are otherwise healthy. In the United States, chronic wounds affect over 6.5 million patients. An estimated excess of $25 billion is

Address correspondence to: Chandan K. Sen, PhD, 473 West 12th Avenue, 512 DHLRI, The Ohio State University Medical Center, Columbus, Ohio 43210, Tel. 614 247 7658; Fax 614 247 7818, chandan.sen@osumc.edu.

Conflict Disclosure: None of the authors have any conflict of interest. We acknowledge that unrestricted research funds were given to the University by the Southwest Technologies.

spent annually on treatment of chronic wounds (1). The burden is also rapidly growing due to increasing health care costs, an aging population, and a sharp rise in the incidence of diabetes and obesity worldwide (1). The research firm Kalorama Information projects the annual wound care products market to reach $21 billion in 2015 from $16.8 billion this year (2). With the cost of chronic wound care sharply rising, efforts are under way to find simple and inexpensive solutions that may be applied to a broad group of affected people.

Ischemia is caused by limited blood supply to the wound-site causing a shortage of oxygen and other blood-borne products required by the tissue to pay for the increased metabolic cost of healing. Peripheral vascular disease or disruption is a common cause of ischemia which may also be viewed as anemia localized to the wound site. Individuals with poor peripheral circulation are at high risk for developing ischemic wounds (1). Other medical conditions also associated with ischemic wounds are diabetes mellitus, renal failure, hypertension, lymphedema, inflammatory diseases such as vasculitis or lupus and current or past tobacco use (3). The porcine model is widely accepted as an excellent preclinical model for human skin wounds (4). In this study, we utilized a well characterized porcine model of chronic ischemic wounds (5).

Collagen is the major constituent of the dermal extracellular matrix (ECM) (6). In addition to providing structural support, collagen dressings support granulation tissue formation by enhancing cellular chemo-attraction, differentiation, and activation (7). Excessive activity of proteolytic enzymes in chronic wounds threatens wound closure by degrading ECM proteins and other bioactive proteins such as growth factors (8). Clinical application of collagen-based products helps manage excessive proteolysis at the wound site favoring healing. The current work builds on our recent report characterizing a modified collagen gel (MCG) dressing for wound care (9). We have earlier reported that MCG improves wound closure in acute excisional wounds (9). Tissue ischemia is a critical component of chronic wound pathology (10). In the current report, we tested the effect MCG on wound angiogenesis using an established preclinical porcine model of experimental chronic ischemic wound (5).

MATERIALS & METHODS

Porcine Ischemic Flap Model

All experiments were approved by The Ohio State University's Institutional LaboratoryAnimal Care and Use Committee (ILACUC). A total of six domestic yorkshire pigs (70–80 lb) were used in this study. Pigs (70–80 lb) were sedated by Telazol and anesthetized by mask with isoflurane (3–4%). The dorsal region was shaved, and the skin was surgically prepared with alternating chlorhexidine 2% and alcohol 70% (Butler Schein, Columbus, OH) scrubs. Four full-thickness bipedicle skin flaps measuring 15 × 5 cm were created on each animal as described before (5). Sterilized silicone sheets (15 × 5 cm) (Technical Products Inc., Decatur, GA) were placed underneath the flaps, and then the flap and silicone sheet edges were sutured to the adjacent skin (Fig. S1A–B). Laser Doppler scanning of the flaps was used to verify blood flow status and degree of ischemia (Fig. S1C).

Wounding and Treatments

A full-thickness excisional wound was created in the center of each flap using an 8 mm disposable biopsy punch. The depth of the wound was measured by the length of stainless steel section of the punch biopsy (8 mm). The wounds were created by cutting through the skin until the entire length of the stainless steel section was below the skin and the plastic shoulders (edges) of the biopsy punch were at the surface of the skin. That length was adequate to reach the subcutaneous fat in all wounds. Excisional wounds on one side were treated with a modified collagen gel (MCG) followed by dressing with Tegaderm™ (3M, St. Paul, MN). The wounds in the contralateral flaps were covered with Tegaderm™ alone as standard of dressing care (control). Treatment sides were alternated between animals to avoid any side-specific effect. All four flaps were covered with V.A.C. Drape (Owens & Minor, Mechanicsville, VA). Dressing was changed every 5–7 days, and any accumulating wound fluid was drained as needed. On designated time points (day 7 and 21 post-wounding), the entire wound tissue was harvested for subsequent analyses. Animals were maintained on 12h light–dark cycles and were euthanized after the completion of experiments. MCG was provided as Stimulen™ gel by Southwest Technologies Inc. (North Kansas City, MO) (11, 12). According to the manufacturer, the unique formulation of the MCG represents a mixture of 52% collagen of long and short polypeptides along with glycerine, water and fragrance. The MCG is a highly concentrated modified collagen (mainly type I) in a gel form. Recently, we have performed proteomic characterization of the MCG (9).

Laser Doppler Scanning of Blood Flow

The MoorLDI-Mark 2 laser Doppler blood flow scanner (resolution: 256 × 256 pixels in the region of interest; each pixel being an actual measurement) was used to study tissue perfusion (Fig. 1, C). Laser Doppler scanning was performed after the surgical procedure and at day 21 post-wounding.

Histology

Formalin-fixed paraffin-embedded or optimum cutting temperature (OCT)-embedded frozen wound-edge specimens were sectioned. The paraffin sections were deparaffinized and stained with hematoxylin & eosin (H&E), Masson’s trichrome, or Picrosirius red staining using standard procedures. Immunohistochemical staining of paraffin or frozen sections was performed using the following primary antibodies: anti- macrophage, L1 calprotectin (1:400; MAC387; Thermo Fisher Scientific Inc., Waltham, MA), anti-von Willebrand’s factor (vWF) (Dako North America Inc., Carpinteria, CA), anti-Ki67 (1:400, Thermo Fisher Scientific Inc., Waltham, MA), anti-vimentin (Sigma-Aldrich®, St Louis, MO), and anti-CCR2 (1:250; Abcam, Cambridge, MA) after heat- induced epitope retrieval when necessary. Secondary antibody detection and counterstaining were performed as described previously (5).

Imaging

Mosaic images of whole wound sections were collected under 20× magnification guided by MosaiX software (Zeiss, Thornwood, NY) and a motorized stage. Each mosaic image was

generated by combining a minimum of 100 images. Between 7 and 9 high- powered representative areas from mosaic images were quantified for each data time point. Image analysis was performed by employing auto-measure software (Zeiss) for quantitation of the percentage of immuno-histochemical positive areas (expressed as % area). *Confocal Scanning Laser Microscope*: visualization of vascular structures within the wound tissues was achieved by using an Olympus Fluoview FV1000 spectral confocal microscope (Olympus, Pittsburgh, PA) under 1000× magnification, while applying an argon laser. Z-stack images were created by merging serial scans of thick tissue section (20 μm) (9).

Cell Culture

Human THP-1 monocytes (American Type Culture Collection, Manassas, VA) were cultured in RPMI 1640 medium with L-glutamine supplemented with 10% FBS and 1% antibiotic antimycotic (AA) (Gibco, Auckland, NZ), and incubated at 37°C in 5% CO2. To differentiate THP-1 monocytes into macrophages, cells were cultured in RPMI 1640 medium with L-Glutamine supplemented with 10% heat inactivated FBS, 1% AA, and 20 ng/ml phorbol 12-myristate 13-acetate (PMA) (Sigma, St. Louis, MO) as described (13).

Supplementation

THP-1 cells were incubated with or without modified collagen gel (50 mg/mL) for 24 h. RNA was extracted from cell pellets using mirVana RNA isolation kit (Ambion, Austin, TX) according to the manufacturer's instructions (5).

RNA Isolation from wound tissues

Immediately after collection, wound tissue biopsies were rinsed in saline, patted dry and snap frozen in liquid nitrogen. Grinding of the tissues was performed using a 6770 Freezer/Mill® cryogenic grinder (SPEX SamplePrep, Metuchen, NJ). Total RNA from tissue or cultured cells were extracted using mirVana RNA isolation kit (Ambion, Austin, TX) as described (5, 13).

Reverse Transcription and Quantitative Real-time PCR

Tissue mRNA was quantified by real-time or quantitative (Q) PCR assay using the double-stranded DNA binding dye SYBR green-I as described previously (5). The primer set used for the individual genes are listed below. 18s rRNA was used as a reference housekeeping gene.

Human_Mrc-1 F: 5′-CCA GGG CGA AAG CCA GGG TG-3′,

Human_Mrc-1 R: 5′ TTC GGG AGT CGT CGT GGG CT-3′,

Human_IL-10 F: 5′- GCT GCA CCC ACT TCC CAG GC-3′,

Human_IL-10 R: 5′-GAC AGC GCC GTA GCC TCA GC-3′,

Human_β-FGF F: 5′ GAA GAG CGA CCC TCA CAT CAA GCT-3′,

Human_β-FGF R: 5′-TCA GTG CCA CAT ACC AAC TGG TGT A-3′,

Pig_VEGF-A F: 5′-CTC TCT CTT ACT TGT ACT GGT CTT T-3′,

Pig_VEGF-A R: 5′-TTA TTT CAA AGG AAT GTG TGG CG-3′,

Pig_vWF F: 5′-GGC TCT GAT AAG CTG TCC GAG G-3′,

Pig_vWF R: 5′-TTT CGG TCC TGG AGC GAG A-3′,

Pig_CCR2 F: 5′-GCG GGG TCA CCT GGG TGG TA-3′

Pig_CCR2 R: 5′-AGT GGC AGG ACC AGC CCC AA-3′

Pig_ARG1 F: 5′-CCA GTC CAT GGA GGT CTG TCT TAT-3′

Pig_ARG1 R: 5′-TGC TAC TGC CGT GTT CAC CG -3′

Pig_TGF β 1_F: 5′-CGG CCC TTC CTG CTC CTC AT-3′,

Pig_ TGF β 1_R: 5′-TTC CAG CCC AGG TCC TTC C-3′,

Human_COL1A F: 5′-ACG TCC TGG TGA AGT TGG TC-3′,

Human_COL1A R: 5′-ACC AGG GAA GCC TCT CTC TC-3′.

Statistics

Data are reported as mean ± SEM of 6 separate animals as indicated. Since the data were not normally distributed, non-parametric statistics was used. Wilcoxon signed-rank test was used to compare control vs. MCG as the wounds were paired within the individual pigs. The significance level for this study was set at 0.05. All analyses were run using Stata 13.1, StataCorp, College Station, Texas.

RESULTS

The pre-clinical model of chronic ischemic wounds, that had been previously characterized (5), was employed for this study. Full thickness bi-pedicle flaps were surgically created on the back of pigs in such a way that interrupted blood supply from underneath and the sides of the flap (Fig S1). After the procedure, ischemia of flap tissue was confirmed by Laser Doppler imaging of blood flow (Fig. S1B–C). The full thickness excisional wounds established in the middle of the flap rested on the most poorly perfused part of the flap. By harvesting whole wound tissues at day 7 and 21 post-wounding, we were able to study the effect of MCG on both early and late events of wound healing processes (Fig. S1A). Successful mounting of inflammatory response and timely resolution are necessary for proper healing of a wound. As part of investigating the inflammatory response, wound macrophages were identified in wound- edge tissue sections using an antibody against macrophage L1 protein/calprotectin (MAC 387), a marker for swine tissue macrophages (14). Anti-MAC 387 also recognizes other cells such as keratinocytes and PMNs. However, in this case keratinocytes were ruled out using anti-keratin-14 (keratinocyte specific, data not shown), the cells (Mac387) did not co-localized with K14 positive cells, thus excluding keratinocytes. For PMN, the nuclear morphology is very distinct as compared to macrophages. DAPI (nuclear stain, blue) staining confirmed that most of the mac387 positive cells were macrophages. Macrophage infiltration to the wound-edge tissue was significantly increased in ischemic wounds treated with MCG at day 7 post-wounding compared to untreated control wounds (Fig. 1A–B). This finding directed us to further

investigate the effect of MCG on macrophage function *in vitro*. THP-1 derived macrophages treated with MCG displayed up-regulation of Mrc-1 gene expression, which is a marker for (M2) reparative macrophage subtype (Fig. 1C) (15). Furthermore, we observed that MCG potently induced the anti-inflammatory cytokine IL-10 and the growth factor β-FGF gene expression (Fig. 2).

To validate the in vitro finding of increased M2 macrophage marker by MCG, we studied the phenotype of wound macrophage in MCG treated wounds. The expression of M2 macrophage markers Arg-1 and CCR2 was determined in wound tissues (Fig 3A–B). A massive induction in Arg-1 and CCR2 was noted in wound tissue following MCG treatment as compared to standard of care (TD, TegadermTM). Recent studies indicate CCL2-CCR2 axis plays a major role in shaping macrophage polarization (16). In M2c macrophages, IL-10 increases expression of CCR2 and CCR5 (17). An immunohistochemistry co-localization study was performed with anti-L1 (Macrophage, green) and anti-CCR2 (M2c macrophage, red) (Fig. 3C). Increased CCR2 positive macrophages in wound tissue 7d post wounding was observed suggesting that either promotion of M2 macrophages recruitment or increased conversion of wound site macrophages to M2 phenotype. In vitro data demonstrating a direct effect of MCG on macrophages by increasing expression of M2 marker supports the latter proposition i.e., increased conversion to M2 phenotype by MCG.

One of the potent angiogenic factors that promote wound revascularization is vascular endothelial growth factor (VEGF). We observed significant increase of VEGF gene expression at day 7 post-wounding in wound-edge tissue treated with MCG compared to corresponding control (Fig. 4A). In concordance with that observation, higher abundance of endothelial cell marker von Willebrand's Factor (vWF) was detected in wound-edge tissues of MCG treated wounds (Fig. 4B). Histological quantitation of endothelial cells abundance in wound-edge tissues showed a markedly elevated count in wounds treated with MCG reflecting increased endothelial cell proliferation (Fig. 4C). MCG-treated ischemic wounds also had markedly higher abundance of endothelial cells 21 days post-wounding indicating that the favorable effect of MCG on endothelial cell proliferation was persistent. Dual immunofluorescence staining technique was employed to co-localize cell-proliferation marker Ki67 within endothelial cells. Ki67 is a nuclear protein that is associated with cellular proliferation (18). Quantitative analysis of Ki67 in vWF+ endothelial cells using an automated software-based methodology revealed that MCG treatment markedly enhanced endothelial cell proliferation at the ischemic wound-edge tissue (Fig. 5). Next, we sought to address the quality and functionality of vascular structures at the wound-edge. Thick wound-edge tissue sections (20 μm) were immuno-stained for vWF and examined using confocal laser scanning microscope (CLSM). Qualitative analyses of wound-edge vascular structures were performed using CLSM by creating Z-stack merged images. Interestingly, on day 21 post-wounding, MCG-treated ischemic wounds displayed more mature and thick vascular formations while control wound-edge tissue featured a scanty distribution of thin vascular structures (Fig. 6A). To determine blood flow, we applied Laser Doppler imaging technology. Laser Doppler scanning is a reliable and applicable method that provides information about tissues' perfusion without physical contact. At day 21 post wounding, scanning of flap tissues by Laser Doppler demonstrated significant increase of blood flow to

wound tissue treated with MCG compared to corresponding control wounds (Fig. 6B). Collectively, MCG-treated ischemic wounds had higher abundance of proliferating endothelial cells which formed mature and functional vascular structures with an increase of blood flow to the wound site.

Fibroblast proliferation is a key driver of the proliferative phase of wound healing. Fibroblasts synthesize collagen and other extracellular matrix components which form the scaffold necessary for the migration and proliferation of other cell types involved in wound repair. Vimentin has been used routinely as a marker for dermal fibroblasts (19,20). Vimentin is one of the intermediate filaments expressed in cells of mesenchymal origin. Other cells of mesenchymal origin such as pericytes may express vimentin. Immunofluorescence staining data revealed that vimentin expression in MCG-treated ischemic wounds was significantly higher on day 21 post-wounding compared to untreated wounds (Fig. 7A–B). Furthermore, on day 7 post-wounding, wound-edge tissue samples from MCG treated group showed up-regulation of TGF-β gene expression compared to corresponding control wounds (Fig. 7C). TGF-β is one of the regulatory growth factors that contribute to fibroblasts' recruitment and stimulation of collagen expression in healing wounds (21). These two findings, along with cyto- morphological properties of vimentin-positive structures, point to the conclusion that MCG-treated ischemic wounds were heavily populated by fibroblasts on day 21 post- wounding. Appropriate collagen deposition helps build tensile strength of the nascent tissue. Histological characterization of collagen in pair-matched wounds was performed through Masson's Trichrome and Picrosirius red staining (PRS). Masson's Trichrome staining of wound-edge tissues showed higher deposition of mature collagen fibers in MCG-treated ischemic wounds (Fig. 8A). PRS was used to identify both types I and III collagen fibers at the wound site (22). In tissues stained with PRS, type I collagen (thick fibers) is viewed as yellow-orange birefringence while type III (thin fibers) is viewed as green birefringence under polarized light microscope. Significant increase of collagen type I: III deposition was noted in MCG-treated wounds (Fig. 8B). This histological phenotypic change was supported by up-regulation of collagen type I gene expression in MCG-treated ischemic wounds in day 7 wound tissue samples (Fig. 8C).

DISCUSSION

Management of ischemic tissue ulceration represents a substantial clinical challenge (23). Excessive proteolysis at the wound site results in uncontrolled degradation of the extracellular matrix (ECM) and growth factors which are essential for normal tissue repair (8). From a clinical point of view, collagen-based products are safe and easily applicable wound dressings that can be combined with other modalities (24). The mechanism of action of collagen-based products is poorly understood. Exogenous collagen to wounds has been shown to promote hemostasis and chemotaxis (25). In addition, collagen dressings act as matrices for new cell ingrowth (25). The current report for the first time demonstrates efficacy of MCG, a collagen based dressing, in the harsh environment of ischemic wounds by resolving inflammation and promoting wound angiogenesis.

Failure to resolve inflammatory state in a timely manner eventually leads to tissue necrosis with increased risk of serious complications such as secondary infection and amputation. A

unique feature of collagen-based products is that they are effective in managing excessive proteolytic enzyme activity (26). Furthermore, exogenously added collagen is claimed to replenish the wound site ECM, thereby providing a scaffold for cell recruitment and migration (25). Interactions between the ECM molecules and cell surface receptors regulate cellular and molecular events of the proliferative phase including epithelialization, angiogenesis, and fibroplasia (27). Wound-site macrophages represent key drivers of wound repair in the inflammatory phase (13). Monocytes recruited to injury site differentiate to pro-inflammatory macrophages (M1) or anti- inflammatory/pro-angiogenic macrophages (M2) (28). The M1 macrophages are responsible for clearing of infectious agents through secretion of pro-inflammatory cytokines and chemokines that stimulate the immune response. A switch from pro- inflammatory to anti-inflammatory macrophage phenotypes occurs following engulfment of apoptotic inflammatory cells also known as efferocytosis (29). M2 macrophages help resolve inflammation in a timely manner and induce granulation tissue formation through enhancing ECM synthesis, angiogenesis, fibroblast proliferation, and epithelialization (30). Imbalance between pro- and anti-inflammatory signals in the direction of the former results in persistent wound inflammation and failure to enter the reparative phase of healing (31). Higher M1:M2 macrophage ratio results in wound chronicity (32). Our recent work demonstrates that macrophage dysfunction with persistent pro-inflammatory signaling is responsible for chronicity of diabetic wounds (29). MCG enhanced macrophage recruitment to the ischemic wound site in the early phase is indicative of a strong inflammatory response. Mrc-1(mannose receptor c) expression is recognized as a marker for the M2 macrophage phenotype (15). Increased CCR2 is a marker for IL-10 induced M2c macrophages (33). We recognize that increased expression of one M2c macrophage (CCR2) in MCG treated wounds does not conclusively demonstrates that MCG promotes M2 macrophage switching. However, this evidence along with in vitro finding on isolated macrophage (Mrc-1) and increased expression of M2 macrophage markers (Arg-1 and CCR2) strongly suggests a potential role of MCG in macrophage polarization in wounds. IL-10 is a major anti- inflammatory agent that helps execute scar-minimized regenerative healing of fetal wounds (34). β-FGF is a key growth factors that promotes granulation tissue formation and wound closure through stimulation of wound angiogenesis, fibroblasts proliferation, and migration (35). Ischemic wounds show delayed macrophage recruitment to the wound site (5). Taken together, the current study demonstrates that even under conditions of ischemia, MCG promoted macrophage recruitment to wounds. Furthermore, presence of MCG helped switching of M1 macrophages to M2 phenotype suggesting MCG not only increases macrophage recruitment but also helps in resolution of prolonged inflammation, a characteristics of ischemic wounds (5). Ischemic wounds lack blood borne products such as oxygen, nutrients, and circulating cells that are necessary for the tissue repair process. Enhancing tissue perfusion therefore represents a useful strategy to rescue ischemic wounds. A robust inflammatory response is known to drive wound neo-vascularization. In this context, wound-site macrophages play a major role (36). Macrophages secrete pro-angiogeneic factors such as VEGF (37). Signaling between endothelial cell-surface receptors and ECM molecules, such as collagen, stimulates migration and proliferation of endothelial cells (27). Also, it has been demonstrated that the three-dimensional structure of the collagen matrix helps endothelial cells to organize into mature vascular structures (38). An abundance of proliferating endothelial cells associated

with mature capillary-like structures in MCG-treated wound-edge tissue is indicative of a potent effect of the dressing on wound vascularization. This contention is supported by improved wound- site blood flow data.

Collagen deposition at the site of healing empowers the nascent tissue with tensile strength which helps prevent wound re-opening. Collagen deposition is known to be inadequate in ischemic wounds which accounts for wound dehiscence and failure to close (39). At the wound site, collagen synthesis is primarily contributed by fibroblasts. Of the several factors that determine the recruitment and proliferation of fibroblasts to the wound-site, ECM and growth factors represent major components (21). Transforming growth factor-β (TGF-β) promotes fibroblast migration, proliferation, and collagen production (40). Increased expression of TGF-β together with increased fibroblast abundance in MCG treated ischemic wounds suggested increased collagen synthesis in these wounds. Indeed, abundant mature collagen fibers were identified in MCG-treated. Importantly, collagen type I dominated over collagen type III. Such increased collagen type I:III ratio is crucial for appropriate wound tensile strength to support the growth of vascularized granulation tissue and to prevent dehiscence (41).

In summary, this study provides novel insight into the mechanism of action of a collagen-based dressing as it relates to outcomes of experimental ischemic wounds. Earlier we demonstrated efficacy of collagen based MCG dressing improved inflammatory cell infiltration and angiogenesis in acute excisional wound (9). Using a porcine ischemic wound model, we have reported that such wounds exhibits prolonged inflammatory phase and poor angiogenesis (5). The current study demonstrates that even under conditions of ischemia i.e., oxygen and nutrient deprivation, MCG is effective in bolstering a reparative inflammatory response followed by improved wound vascularization and favorable organization of the extracellular matrix. Taken together, the observations of the current study warrant testing the efficacy of MCG in a clinical setting.

Supplementary Material

Refer to Web version on PubMed Central for supplementary material.

Acknowledgments

The work was supported by National Institutes of Health awards GM077185, GM069589 and DK076566. We thank Dr. Ed Stout and Ms. Angie McKessor Southwest Technologies for providing the dressing and unrestricted research development funding to The Ohio State University. We thank Mr. Gary Phillips, Center for Biostatistics, The Ohio State University for assistance with the statistical analysis for this study.

References

1. Sen CK, Gordillo GM, Roy S, Kirsner R, Lambert L, Hunt TK, et al. Human skin wounds: A major and snowballing threat to public health and the economy. Wound Repair Regen. 2009; 17(6):763–71. [PubMed: 19903300]
2. projects KI. Advanced Wound Care Markets Worldwide (Skin Ulcer, Burns, Surgical/Trauma). 2012.
3. Biswas S, Roy S, Banerjee J, Hussain SR, Khanna S, Meenakshisundaram G, et al. Hypoxia inducible microRNA 210 attenuates keratinocyte proliferation and impairs closure in a murine

model of ischemic wounds. Proc Natl Acad Sci U S A. 2010; 107(15):6976–81. [PubMed: 20308562]

4. Sullivan TP, Eaglstein WH, Davis SC, Mertz P. The pig as a model for human wound healing. Wound Repair Regen. 2001; 9(2):66–76. [PubMed: 11350644]
5. Roy S, Biswas S, Khanna S, Gordillo G, Bergdall V, Green J, et al. Characterization of a preclinical model of chronic ischemic wound. Physiol Genomics. 2009; 37(3):211–24. [PubMed: 19293328]
6. Alberts, B.; Johnson, A.; Lewis, J., et al. The Extracellular Matrix of Animals. New York: Garland Science; 2002.
7. Brett D. Review of collagen and collagen-based wound dressings. Wounds. 2008; 20(12):347–53.
8. Cullen B, Watt PW, Lundqvist C, Silcock D, Schmidt RJ, Bogan D, et al. The role of oxidised regenerated cellulose/collagen in chronic wound repair and its potential mechanism of action. Int J Biochem Cell Biol. 2002; 34(12):1544–56. [PubMed: 12379277]
9. Elgharably H, Roy S, Khanna S, Abas M, Ghatak PD, Das A, et al. A Modified collagen gel enhances healing outcome in a pre-clinical swine model of excisional wounds. Wound Repair Regen. 2013 in Press.
10. Roy S, Khanna S, Rink C, Biswas S, Sen CK. Characterization of the acute temporal changes in excisional murine cutaneous wound inflammation by screening of the wound-edge transcriptome. Physiol Genomics. 2008; 34(2):162–84. [PubMed: 18460641]
11. Anderson, REWC.; Wetzeler, C. Clinical case studies utilizing hydrolyzed collagen powder to effectively heal a variety of wounds. Proceedings of the Symposium on Advanced Wound Care & Wound Healing Society; April 28th – May 1st; Tampa, Florida. 2007.
12. Leslie, SBT. The effect of powdered collagen on chronic wounds. Proceedings of the Clinical Symposium on Advances of Skin & wound Care; September 9th – 12th; National Harbor, MD. 2011.
13. Ganesh K, Das A, Dickerson R, Khanna S, Parinandi NL, Gordillo GM, et al. Prostaglandin E(2) induces oncostatin M expression in human chronic wound macrophages through Axl receptor tyrosine kinase pathway. J Immunol. 2012; 189(5):2563–73. [PubMed: 22844123]
14. Dor FJ, Gollackner B, Kuwaki K, Ko DS, Cooper DK, Houser SL. Histopathology of spleen allograft rejection in miniature swine. Int J Exp Pathol. 2005; 86(1):57–66. [PubMed: 15676033]
15. Martinez FO, Helming L, Gordon S. Alternative activation of macrophages: An immunologic functional perspective. Annu Rev Immunol. 2009; 27:451–83. [PubMed: 19105661]
16. Sierra-Filardi E, Nieto C, Dominguez-Soto A, Barroso R, Sanchez-Mateos P, Puig-Kroger A, et al. CCL2 shapes macrophage polarization by GM-CSF and M-CSF: Identification of CCL2/CCR2-dependent gene expression profile. J Immunol. 2014; 192(8):3858–67. [PubMed: 24639350]
17. Moser B, Loetscher P. Lymphocyte traffic control by chemokines. Nat Immunol. 2001; 2(2):123–8. [PubMed: 11175804]
18. Gerdes J, Lemke H, Baisch H, Wacker HH, Schwab U, Stein H. Cell cycle analysis of a cell proliferation-associated human nuclear antigen defined by the monoclonal antibody Ki-67. J Immunol. 1984; 133(4):1710–5. [PubMed: 6206131]
19. Kim SS, Gwak SJ, Choi CY, Kim BS. Skin regeneration using keratinocytes and dermal fibroblasts cultured on biodegradable microspherical polymer scaffolds. J Biomed Mater Res B Appl Biomater. 2005; 75(2):369–77. [PubMed: 16025446]
20. Radfar AJ, Robbins PD, Huard J, Rosas FR, Dohar JE, Hebda PA. Transplantation of virally transduced cells into the dermis of immunocompetent and immunodeficient (SCID) mice to determine gene expression profile and differential donor cell survival. Wound Repair Regen. 2000; 8(6):503–10. [PubMed: 11208177]
21. Werner S, Grose R. Regulation of wound healing by growth factors and cytokines. Physiol Rev. 2003; 83(3):835–70. [PubMed: 12843410]
22. Montes GS, Junqueira LC. The use of the Picrosirius-polarization method for the study of the biopathology of collagen. Mem Inst Oswaldo Cruz. 1991; 86(Suppl 3):1–11. [PubMed: 1726969]
23. Page CF, Gault WR. Managing ischemic skin ulcers. Am Fam Physician. 1975; 11(2):108–14. [PubMed: 164763]

24. Iorio ML, Shuck J, Attinger CE. Wound healing in the upper and lower extremities: A systematic review on the use of acellular dermal matrices. Plast Reconstr Surg. 2012; 130(5 Suppl 2):232S–41S. [PubMed: 23096978]
25. Seaman S. Dressing selection in chronic wound management. J Am Podiatr Med Assoc. 2002; 92(1):24–33. [PubMed: 11796796]
26. Rangaraj A, Harding K, Leaper D. Role of collagen in wound management. Wounds UK. 2011; 7(2)
27. Davis GE, Senger DR. Endothelial extracellular matrix: Biosynthesis, remodeling, and functions during vascular morphogenesis and neovessel stabilization. Circ Res. 2005; 97(11):1093–107. [PubMed: 16306453]
28. Gordon S, Taylor PR. Monocyte and macrophage heterogeneity. Nat Rev Immunol. 2005; 5(12): 953–64. [PubMed: 16322748]
29. Khanna S, Biswas S, Shang Y, Collard E, Azad A, Kauh C, et al. Macrophage dysfunction impairs resolution of inflammation in the wounds of diabetic mice. PLoS One. 2010; 5(3):e9539. [PubMed: 20209061]
30. Xu W, Roos A, Schlagwein N, Woltman AM, Daha MR, van Kooten C. IL-10- producing macrophages preferentially clear early apoptotic cells. Blood. 2006; 107(12):4930–7. [PubMed: 16497970]
31. Eming SA, Krieg T, Davidson JM. Inflammation in wound repair: Molecular and cellular mechanisms. J Invest Dermatol. 2007; 127(3):514–25. [PubMed: 17299434]
32. Sindrilaru A, Peters T, Wieschalka S, Baican C, Baican A, Peter H, et al. An unrestrained proinflammatory M1 macrophage population induced by iron impairs wound healing in humans and mice. J Clin Invest. 2011; 121(3):985–97. [PubMed: 21317534]
33. Mantovani A, Sica A, Sozzani S, Allavena P, Vecchi A, Locati M. The chemokine system in diverse forms of macrophage activation and polarization. Trends Immunol. 2004; 25(12):677–86. [PubMed: 15530839]
34. Liechty KW, Kim HB, Adzick NS, Crombleholme TM. Fetal wound repair results in scar formation in interleukin-10-deficient mice in a syngeneic murine model of scarless fetal wound repair. J Pediatr Surg. 2000; 35(6):866–72. discussion 72–3. [PubMed: 10873028]
35. Kanazawa S, Fujiwara T, Matsuzaki S, Shingaki K, Taniguchi M, Miyata S, et al. bFGF regulates PI3-kinase-Rac1-JNK pathway and promotes fibroblast migration in wound healing. PLoS One. 2010; 5(8):e12228. [PubMed: 20808927]
36. Naldini A, Carraro F. Role of inflammatory mediators in angiogenesis. Curr Drug Targets Inflamm Allergy. 2005; 4(1):3–8. [PubMed: 15720228]
37. Willenborg S, Lucas T, van Loo G, Knipper JA, Krieg T, Haase I, et al. CCR2 recruits an inflammatory macrophage subpopulation critical for angiogenesis in tissue repair. Blood. 2012
38. Montesano R, Orci L, Vassalli P. In vitro rapid organization of endothelial cells into capillary-like networks is promoted by collagen matrices. J Cell Biol. 1983; 97(5 Pt 1):1648–52. [PubMed: 6630296]
39. Schwarz DA, Lindblad WJ, Rees RR. Altered collagen metabolism and delayed healing in a novel model of ischemic wounds. Wound Repair Regen. 1995; 3(2):204–12. [PubMed: 17173649]
40. Cordeiro MF, Bhattacharya SS, Schultz GS, Khaw PT. TGF-beta1, -beta2, and – beta3 in vitro: biphasic effects on Tenon's fibroblast contraction, proliferation, and migration. Invest Ophthalmol Vis Sci. 2000; 41(3):756–63. [PubMed: 10711691]
41. Hurme T, Kalimo H, Sandberg M, Lehto M, Vuorio E. Localization of type I and III collagen and fibronectin production in injured gastrocnemius muscle. Lab Invest. 1991; 64(1):76–84. [PubMed: 1703587]

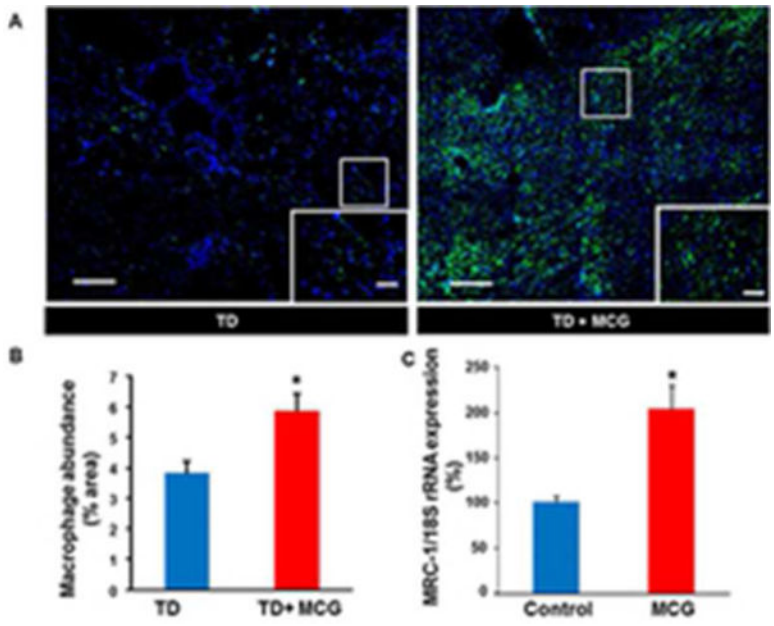

Figure 1. Increased recruitment of macrophage to ischemic wounds treated with MCG

(A) Representative mosaic images of wound-edge tissues that were immunostained using Anti-MAC387 (macrophages, green). The sections were counterstained with DAPI (blue). Scale bar, 200 μm. Insets are zoomed regions in the image, Scale bar, 50 μm. TD, Tegaderm™; MCG, modified collagen gel. (B) Bar graph shows quantitation of macrophage infiltration at day 7 post-wounding in ischemic wounds treated or untreated with MCG. Data are presented as mean ± SEM (n= 6); *p <0.05 compared to untreated wounds. (C) Up-regulation of macrophage mannose receptor 1 (MRC-1) gene expression in THP-1 differentiated human macrophages treated with modified collagen gel (MCG) for 24h. MRC-1 gene expression was measured using quantitative real-time PCR. Data are presented as % change compared to untreated cells. Data are mean ± SEM (n = 4); *p < 0.05.

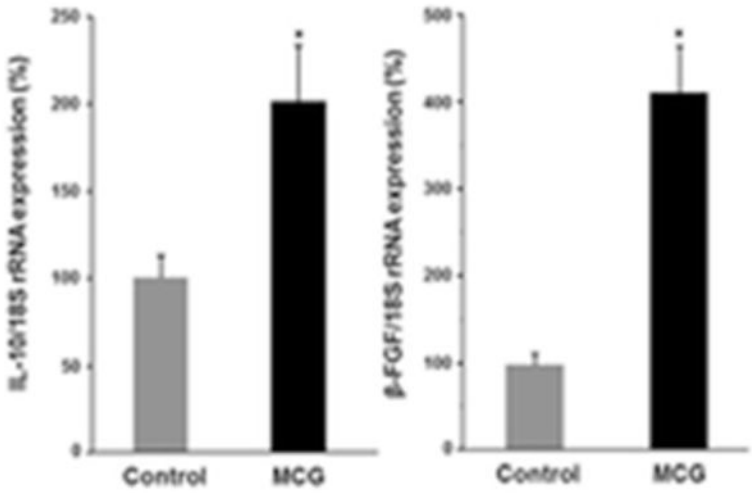

Figure 2. Induction of IL-10 & β-FGF genes by modified collagen gel (MCG)

Up- regulation of IL-10 & β-FGF gene expression in THP-1 differentiated human macrophages treated with modified collagen gel (MCG) for 24h. The expressions of mRNA for IL-10 and bFGF were determined using quantitative real-time PCR. Data are presented as % change compared to untreated cells. Data are mean ± SEM ($n = 4$); *$p < 0.05$.

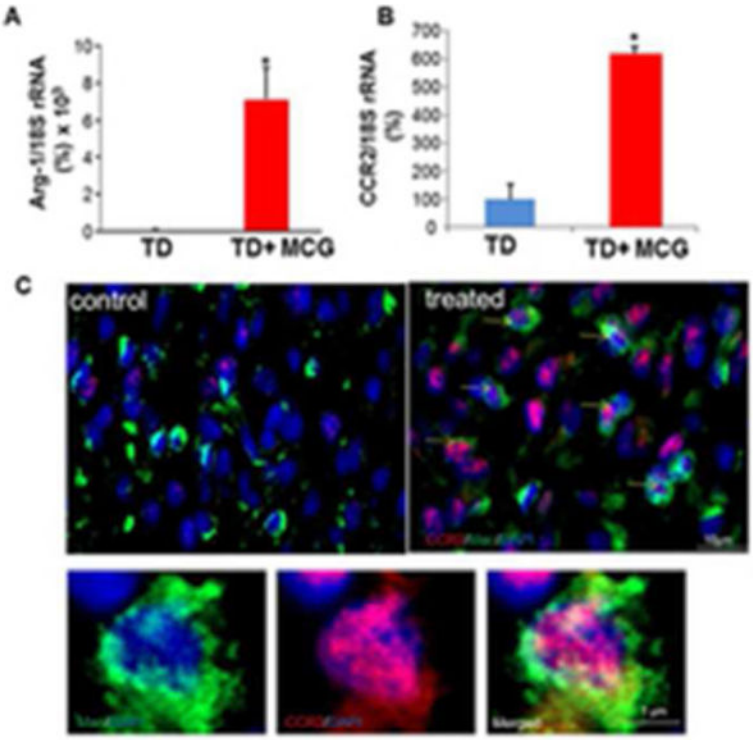

Figure 3. increased CCR2 (M2c macrophage marker) expression in macrophages treated with modified collagen gel (MCG)

(A&B) Real-time PCR was used to measure Arg-1 & CCR2 gene expressions in wound tissue samples at day 7 post- wounding. Gene expression data are presented as % change compared to untreated wound tissues. Data are mean ± SEM; *$p < 0.05$. (C) Representative images of control and treated wound-edge tissues immunostained using Anti-MAC387 (macrophages, green) and Anti-CCR2 E68 (M2c macrophages, red). The sections were counterstained with DAPI (blue). Scale bar, 10 μm. Insets are zoomed regions in the image, Scale bar, 1 μm.

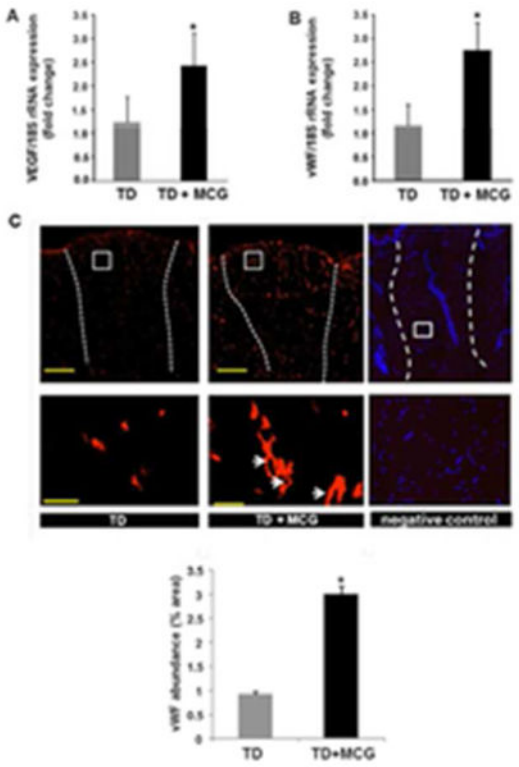

Figure 4. Modified collagen gel (MCG) promotes vascularization of ischemic wounds

(A&B) Total RNA was isolated from wound-edge tissue material stored in liquid nitrogen. Real-time PCR was used to measure VEGF & vW F gene expressions in samples at day 7 post-wounding. Gene expression data are presented as % change compared to untreated wound tissues. Data are mean ± SEM ($n = 6$); *$p < 0.05$. (C) Representative immunofluorescence images from wound sections stained with von Willebrand Factor (red). Scale bar, 500 μm. Lowed panel are zoomed regions in the images on top, Scale bar, 50 μm. Negative control image shows specificity of the anti- vWF staining. The section was counterstained with DAPI (blue, nuclear) to show the cells present in the section. Bar graph shows quantitation of the endothelial cells in MCG-treated or untreated ischemic wounds at day 21 post-wounding. Data are presented as mean ± SEM ($n = 6$); *p <0.05 compared to untreated wounds. White dashed lines indicate the edges of the wound.

TD, Tegaderm™; MCG, modified collagen gel.

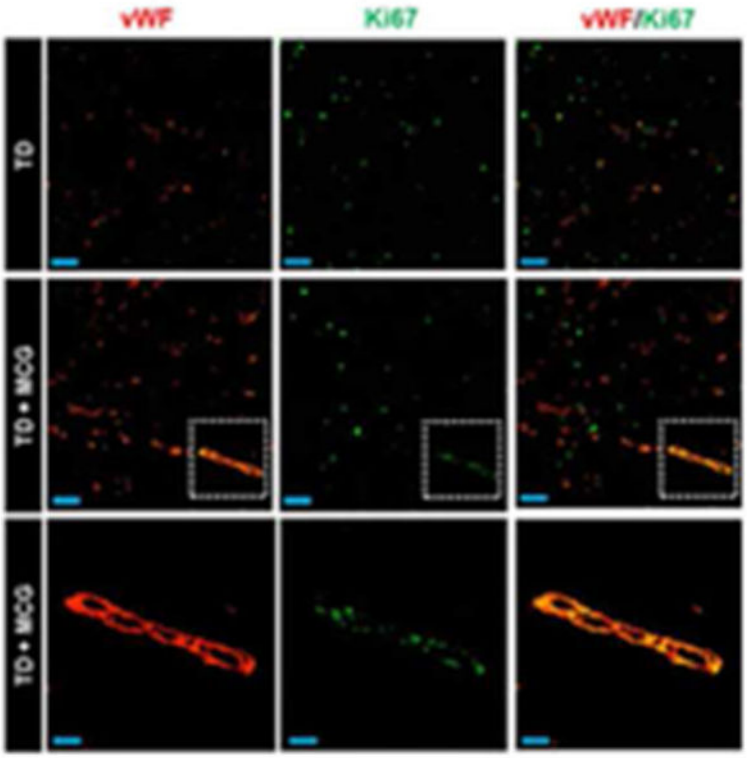

Figure 5. Vascularization of MCG-treated ischemic wounds was enhanced by endothelial cell proliferation

Representative immunofluorescence images of wound sections (8 μm) at day 21 post-wounding stained using Ki67 (marker of proliferating cells, green) and von Willebrand Factor (endothelial cells, red) antibodies. A marked increase of proliferating endothelial cells in MCG-treated ischemic wounds compared to control wounds as evident by co-localization of Ki67 within vascular structures (yellow areas in merged images) was noticed. The bottom panels are zoomed regions within the dashed white boxes in the corresponding middle panels. Top and middle panels scale bars, 50 μm. Bottom panel scale bar, 20 μm.

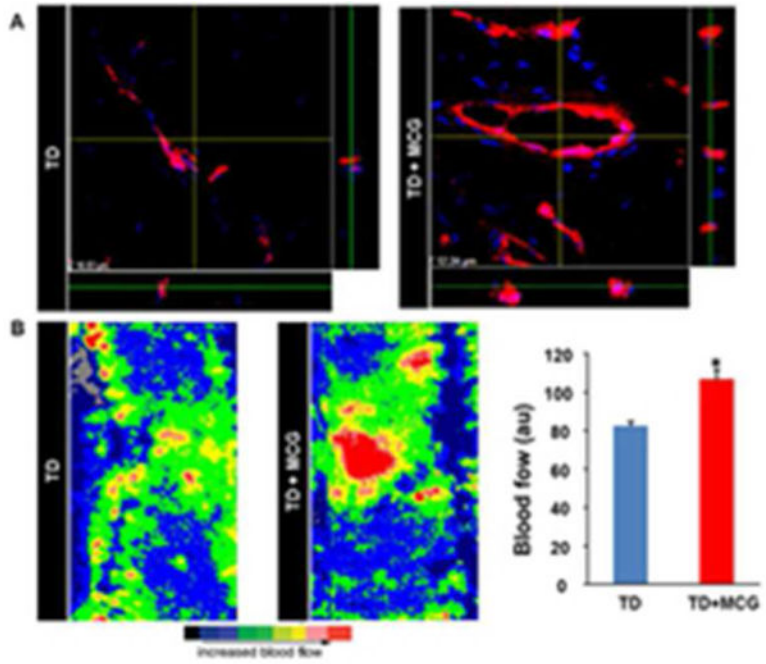

Figure 6. Vascularization of MCG-treated ischemic wounds displayed improved maturity and functionality

(A) Wound tissue sections immunostained with an antibody against von Willebrand Factor (red) followed by counterstaining with DAPI (blue),viewed with a confocal laser scanning microscopy at a 1000× magnification. Z- stack images were created by merging serial scans of thick tissue section (20 μm). Note increased mature vascular structures in MCG-treated ischemic wounds compared to untreated wounds in the x/y plane, whereas the x/z and y/z planes display the thickness of the vascular structures in the tissue section. (B) Laser Doppler images of ischemic flaps on the back of the pig at day 21 post-wounding. Marked increase in blood flow (red) was noted in ischemic wounds treated with MCG. Bar graph represents the quantitative data from Laser Doppler analysis. Data presented as mean ± SEM (n = 6); *p <0.05 compared to untreated wounds.

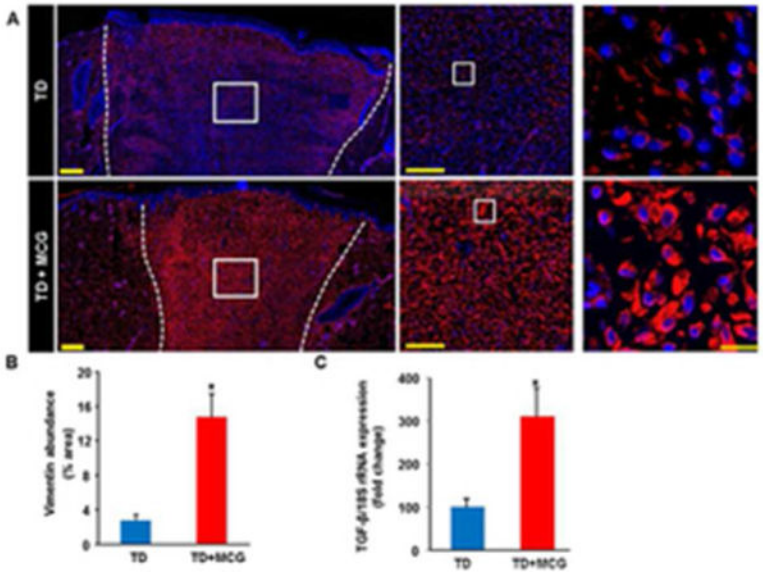

Figure 7. Increased vimentin expression in ischemic wounds treated with modified collagen gel (MCG)

(A) Mosaic images of wound tissue sections that were immune-stained with anti-vimentin (red) and DAPI (blue). White dashed lines indicate the edges of the wound. Middle and Right panels are zooms of the boxed areas within the images in the left panels. Scale bar,100 μm (middle); Scale bar,10 μm. (B) Bar graph shows quantitation of vimentin expression at day 21 post-wounding in MCG- treated or –untreated ischemic wounds. Data are presented as mean ± SEM (n = 6); *p <0.05 compared to untreated wounds. (C) Real-time PCR was used to measure TGF-β gene expression in wound tissue samples of day 7 post-wounding. Gene expression data are presented as % change compared to untreated control wound tissues. Data are mean ± SEM (n = 4); *p <0.05.

TD, Tegaderm™; MCG, modified collagen gel.

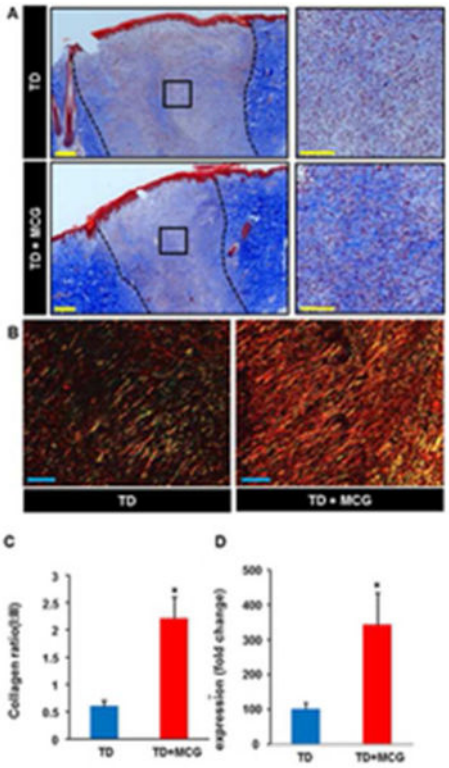

Figure 8. Increased mature collagen deposition in ischemic wounds treated with modified collagen gel (MCG)

(A) Representative images of formalin-fixed paraffin- embedded (FFPE) wound biopsy sections (5 μm) stained using Masson's Trichrome. This staining results in blue-black nuclei, blue collagen, and light red or pink cytoplasm. Epidermal cells appear reddish. Scale bar, 200 μm. Black dashed lines indicate the edges of the wound. Right panels are the zooms of the boxed areas within the images in the left panels. Scale bar, 100 μm. Bar graph shows quantitation of collagen abundance in MCG-treated or –untreated ischemic wounds on day 21 post- wounding. Data are presented as mean ± SEM (n = 6); *p <0.05 compared to untreated wounds. (B) Representative images from FFPE wound tissue biopsy sections stained using picrosirius red staining (PRS). This stain can be used to distinguish between type I and type III collagen in wound tissues; type I (thick fibers) appears yellow-orange birefringence while type III (thin fibers) appears green birefringence when viewed under polarized light microscope. Showing is a marked increase of collagen I:III ratio (yellow-orange fibers to green fibers) in MCG-treated ischemic wounds compared to untreated control wounds. Scale bar, 100 μm. (C) Collagen type I gene expression in day 7 ischemic wound tissues was quantified using real-time PCR. Gene expression data are presented as % change compared to MCG-untreated control wound tissues. Data are mean ± SEM (n = 6); *p < 0.05.